Baseline Tracking in Bipolar Charge Signal Process by Dynamic Time Warping Algorithm

Yang Jiang, Tong Deng, and Karim M. Nasr, *Senior Member, IEEE*

***Abstract*—Electrostatic charge of solid particles can cause problems in many handling processes and need to be evaluated in terms of charge levels and charge polarity. An inductive charge sensor is suitable for the evaluation of both levels and distributions of particle charges at the same time. However, the performance of charge sensing is critically subject to its signal process, which can result in huge errors. One of error sources is drifting of the baseline tracked, which leads raw signals generated by the sensor to be distorted. Especially in determining polarity and quantity of bipolar charges, the distorted signal leads to significant biases and errors in charge measurements, when the number of particles measured is big. Currently, the existing correction algorithms cannot produce a satisfied result in baseline tracking. In this paper, the baseline drifting problem for the charge signals has been explored according to the types of charge polarity. For unipolar charge signals, charge polarity and quantity are determined directly by a poles-pairing method without any further baseline correction. For bipolar charge signals, a new method in baseline tracking and correction has been developed based on dynamic time warping algorithm. Further optimization by a double-check process is used to remove the 'small hump' errors in the signal. With the results of the charge measurements, this new method shows significant advantages on accuracy and efficiency of charge detection compared to the other existing methods.**

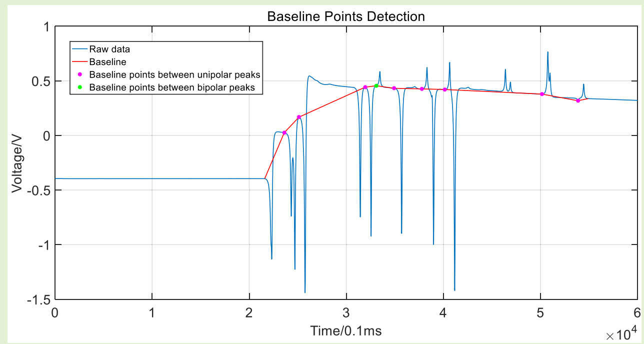

***Index Terms*—Electrostatic charge, inductive sensor, signal restoration, baseline tracking, dynamic time warping.**

I. Introduction

ELECTROSTATIC charge generated in powder processing is popular in many industries, especially in pharmaceutical and metallurgical industries whereas particles experience the friction between particles and container wall during mixing, blending and transportation [1]. Static charge on particles can cause severe problems such as agglomeration, segregation, adhering to the equipment, or even fire explosion [2], [3]. Even if the problems are not so severe, levels of charge and charge polarity can influence material characteristics such as size of agglomeration, which shows that proper assessments of particle charge are necessary for process control [4].

Traditionally, many methods have been used to detect charge behaviour and charge levels of powders, but none of them can rapidly obtain charge distributions among the particles except inductive charge sensors [5]–[8]. The principle of an inductive charge sensor developed at the Wolfson Centre is shown in Fig. 1 [9], where the particles are fed by a vibrating feeder into a ring-shaped sensor. When a charged particle passes through the sensor ring, the charge on the particle generates an image charge on the ring, which produces an induced current in the sensor. The induced current is integrated by a pure integrator and converted to a voltage signal so the charge for the particle can be detected. For a single particle, the charge (Q) is subject to the voltage induced and the capacitance of the feedback capacitor in the integrating circuit, which can be obtained by:

$$\mathrm{Q} = C_{\mathrm{INT}} \Delta V \, \mathrm{G}/(1+\mathrm{G}) \tag{1}$$

where $\mathrm{C_{INT}}$ is the capacitance of the feedback capacitor, G is the gain of the amplifier circuit, and ΔV is the absolute voltage induced by the charged particle.

With series charged particles passing through the sensor (electrode), a sequence of voltage impulses generated by the particles in time domain represents the particle charges. Total charge for all particles is obtained by accumulating the charges on individuals so charge levels and polarity can be detected by averaging the charge over the mass of the particles and impulse direction respectively. A typical signal is shown in Fig. 2.

To process the charge from the signal in Fig. 2, it faces a few challenges: identifying peak and peak direction, baseline drifting and noise reduction, where the baseline is the signal output without any charged particles passed through the sensor.

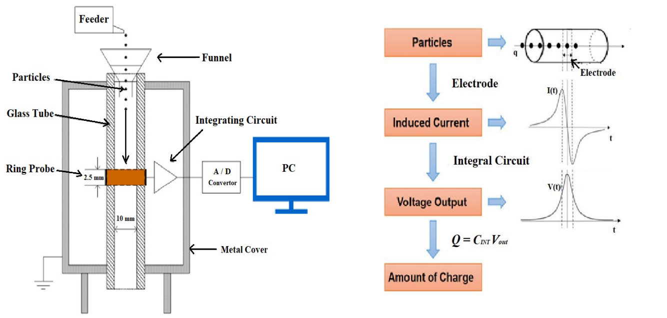

Fig. 1. Schematic overview of an inductive charge sensor and the principle of charge measurement by scanning charged particles.

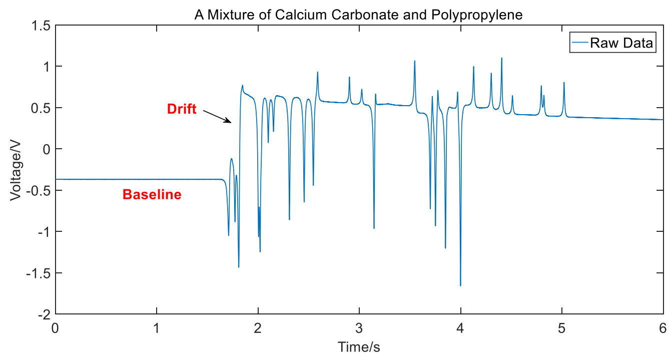

Fig. 2. A typical charge signal from inductive sensor which contains noise and baseline drifting.

The baseline is important for calculating the charge by Eq. (1) as the ΔV is the absolute value between the baseline (before particle entering) and peak value (particle at the centre of the ring sensor). So, baseline tracking in signal process is critical for charge measurement of an inductive sensor.

To process it in a computer, baseline tracking can be really challenged using an algorithm because of the baseline drifting, which refers to that a charge signal deviates from non-charged position and fluctuates slowly up and down due to charge remaining in the sensor and slow charge dissipated. Such fluctuations prevent further peak detection in waveform correctly. Based on a review of the existing baseline tracking and correction methods, a new solution is introduced in this paper for different types of charges. For unipolar charges, change polarity and quantity are determined directly by a poles-pairing method without further baseline correction, but for bipolar charges a new baseline correction method based on dynamic time warping algorithm is developed with a further optimization by a repeat process (check on signal sharpness).

II. Related Works and the Problems

Signal drifting is common in many sensors, which causes linear or nonlinear changes in the overall trend of signals and disturbs the useful signals, especially amplitude measurements of signals [10], [11]. For inductive charge signals, Hussain [9] argued that the reason for that was the particle concentration. Because the charge amplifier connected to the sensor was essentially an integrator, a time was needed to integrate the impulses generated by a single particle. When multiple particles passing through the sensor, the remained charges might saturate the electronic equipment and created signal drifting. Similarly, smaller particles were more likely to produce signal drifting than large ones, because large particles had better dispersion characteristics and more spacing between the particles in the sensor. Through comparative experiments, the effect of particle concentration and particle size on baseline drifting was demonstrated. Common methods to track baseline in literature can be classified into three categories: filters, wavelet transform and curve fitting in signal process.

Using a filter to remove baseline drifting is to eliminate the low-frequency components in the signal through a high-pass filter, *i.e.*, to erase the trend of slow changes in the signal. Sigurdsson *et al.* [12] believed that a high-pass filter could indeed reduce the large-scale displacement and distortion of the waveform. However, it still led to a loss of low-frequency components in the data, because sometimes it was impossible to determine the frequency range of interest. Similarly, Maess *et al.* [13] argued that a high-pass filter was not an alternative to de-trending or even baseline correction, and that a criterion should be established to identify the distortion caused by filter.

Baseline correction by wavelet transform functions was consistent with that of removing drifting by filter, *i.e.*, removing the non-drastic changing components from the signal. The signal was firstly decomposed to remove the baseline with the wavelet transform. Daubechies and Symlet were the two commonly used mother wavelets [14]. After proper decomposition, an approximate coefficient was obtained from the low-frequency part of the signal, and the detail coefficient was derived from the high-frequency part of the signal. It was believed that the baseline was related to the approximate coefficient [15]. However, like the filter method, the wavelet transforms arbitrarily assumed that the baseline was separated from the rest of the signal. Moreover, for some cases that the baseline drifting was much larger than the scale of the signal, the decomposition level of the data was not enough, and a deeper decomposition was usually required [16].

Curve fitting was a more popular method compared to the others. It reduced the loss of low-frequency components of the signal to some extent. By this method, the baseline was fitted to a N-order polynomial, thereby removing it from the signal. The conventional curve fitting methods were polynomial fitting and spline fitting based on least-squares criterion [17]–[19]. As a mathematical optimization technique, the least square criterion sought the optimal function matching of data by minimizing the sum of squares of errors. Since the curve fitting method required user inputs to select a subset of points on the signal for fitting, although there were satisfactory results under the premise of an accurate selection of points, it still contained too much subjective judgment and would be a laborious task for a large amount of data.

Moreover, Pang *et al.* [20] used nonlinear morphological filtering to achieve the purpose by selecting appropriate structural elements for expansion and corrosion operations. The result gave a higher signal-to-noise ratio and a minimum mean square error, but it was challenging to choose a right structural element. For curve fitting, non-quadratic criteria were used by Mazet *et al.* [21] to determine polynomial coefficients at a better match. It could have a better fit, but an appropriate cost function needed to be selected manually, and the user's subjectivity might cause a wrong fitting.

All the baseline tracking methods described above focused on an overall signal, and getting a general trend of the waveform, and then eliminated the trend, while retaining the signal component that changed dramatically. In other words, these methods obtained a baseline first and then found the starting

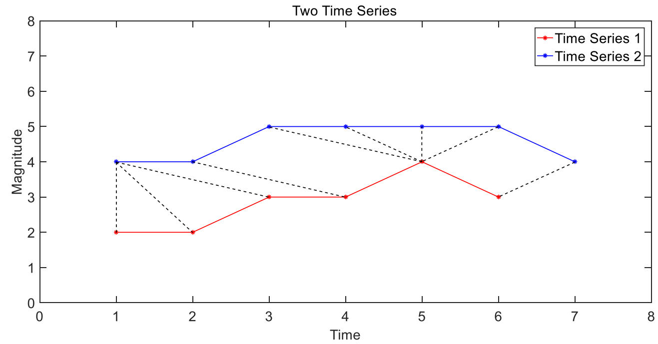

Fig. 3. Two time series signals ×1 and ×2 for the similarity of the time series.

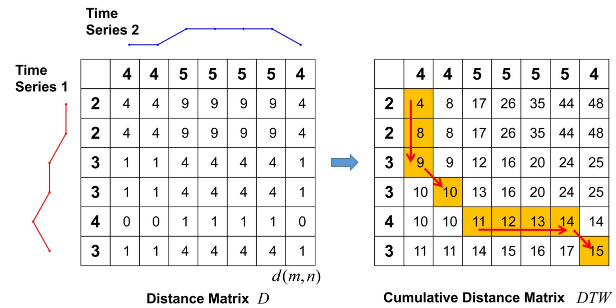

Fig. 4. The distance matrix and cumulative distance matrix for ×1 and ×2 showing the shortest warping path.

point (baseline point) for every signal of interest on that line, which was a holistic to local approach. The methods could quickly locate a general trend as a baseline but had difficulties to prove that the baseline point was on the line or not.

Instead, a new local to holistic baseline tracking method developed in this study can identify some obvious baseline points with high accuracy first, and then obtain a baseline to orient the whole signal based on these points. By the way, most the obvious points in the waveform can be secured accurately, and the other points can be obtained with the assistance of the obvious ones. This method works based on individual peaks in the signal. In case of unipolar and bipolar charges, baseline tracking solutions can be different. For unipolar charge signals, a subtraction method is used in the study to simplify the problem by calculating amplitude of peaks directly without using the new method. Given the complexity of bipolar charge signals, the new local to holistic baseline tracking method is used to find the baseline points first and then derive a baseline. To locate the baseline points, a threshold method is developed based on the dynamic time warping (DTW) algorithm [22]. The new mothed provides a better accuracy to locate the baseline points and minimizes errors of the wrong points on the line.

III. Dynamic Time Warping Algorithm

Dynamic time warping (DTW) algorithm is an algorithm to measure the similarity between two time series, especially for time series with different lengths, *e.g.*, audio signals of different people reading the same word [23], [24]. DTW algorithm calculates the similarity of time series of different lengths by extending and shortening them, as shown in Fig. 3, two time series (solid lines) and their similarity (dotted lines) with corresponding points on the solid lines.

The DTW algorithm measures the similarity between two time series using the sum of the distances between all corresponding points, which is called the warp path distance. For example, $Q = q_1, q_2, \ldots, q_i, \ldots, q_n$ and $C = c_1, c_2, \ldots, c_j, \ldots, c_m$ are two time series with different lengths, an $m \times n$ distance matrix D (shown in Fig. 4) needs to be established for the dynamic programming algorithm. The matrix element $d(q_i, c_j)$ represents the distance between q_i and c_j. The Euclidean distance is generally used, $d\ (q_i, cj) = (q_i - c_j)^2$

Briefly, this algorithm is looking for the shortest path through several elements in the matrix, and the elements that the path passes through are the corresponding points when the two series are compared. After obtaining the distance matrix, a cumulative distance matrix (loss matrix) *DTW* (Fig. 4) is generated according to the continuity and monotonicity principle of the dynamic programming algorithm. In the cumulative distance matrix, the element can be expressed as:

$$\begin{aligned} DTW(1,1) &= D(1,1) \\ DTW(1,j) &= D(1,j-1) + d(q_1, c_j) \\ DTW(i,1) &= D(i-1,1) + d(q_i, c_1) \\ DTW(i,j) &= d(q_i, c_j) + \min\{DTW(i\text{-}1, j), \\ &\qquad DTW(i\text{-}1, j\text{-}1), DTW(i, j\text{-}1)\} \end{aligned} \tag{2}$$

In Eq. (2), d is the distance between q_i and c_j. *DTW* is the sum of the Euclidean distance of the current position and the minimum of the adjacent three cumulative distances. *DTW (m, n)* is the warp path distance, which is the shortest distance between two time series. In Fig. 4, by tracking from *DTW (1, 1)* to *DTW (m, n),* the shortest warping path can be obtained.

Dynamic time warping algorithms have been used in biomedical applications, such as recognition, classification, and extraction of ECG signals [24], [25]. Because of its flexibility in template matching, it is used most often in voice recognition [26].

IV. Methodology for Baseline Tracking

A. Baseline Tracking for Unipolar Charge Signals

For the unipolar charge signal, all signal peaks generated by charges have the same polarity direction (see Fig. 5). In a unipolar charge signal, the amplitude of a peak is the vertex of each peak, *i.e.*, the difference between baseline point and the peak represented by red dots in the figure. The starting point of the peak is where the signal starts to change and is represented by green points. Since all peaks in the signal are in the same direction, the true magnitude of a peak is vertical distance between the starting point and the ending point. It means that by finding these points, the true amplitude can be obtained without any baseline correction.

To find out the starting and ending points of the peaks, the peaks must be detected first. Taking each bit of a signal ***S***, if *s(i)>s(i+1)* and *s(i)>s(i-1)*, the value $s(i)$ is the maximum point. If *s(i)<s(i+1)* and *s(i)<s(i-1)*, the $s(i)$ is the minimum point. After identifying all the peaks, the true magnitudes are formed by pair positive and negative peaks.

For positive charges, the peaks of a magnitude always start with a minimum point and end at a maximum point on the timeline. For negative charges, they are opposite. In practice,

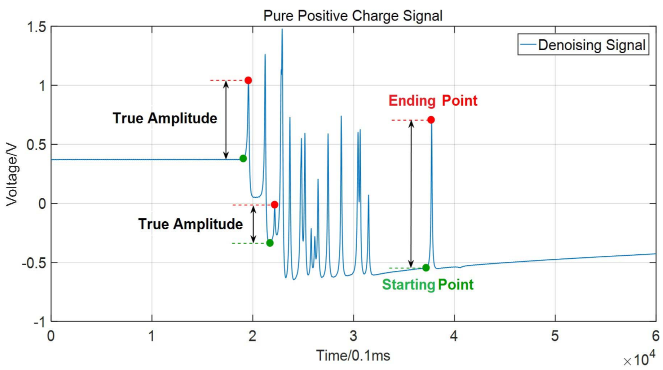

Fig. 5. A unipolar charge signal and true amplitudes in the signal.

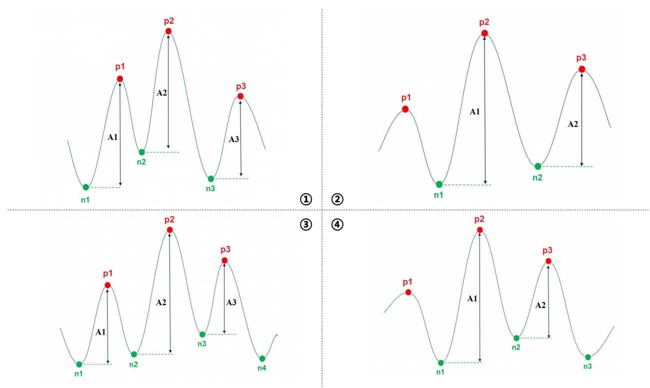

Fig. 6. Four cases of pole distribution.

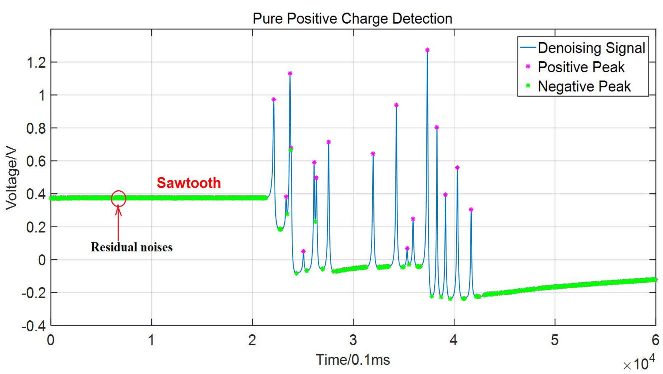

Fig. 7. Indiscernible teeth in the waveform.

the peak points in charge signals may be not in pairing or the signal starts with different type of peaks (maximum or minimum point) (Fig. 6 (2) and (3)), this will lead to some errors in peak detection. To solve the problem, any signals can be classified in four categories as shown in Fig. 6 as paired peaks (case of (1) and (4)) and unpaired peaks (case of (2) and (3)). With the categories, the distribution of peaks in the signal is checked and classified. Then the positive and negative peaks are paired according to their categories to form the true amplitudes.

Since any charge signals have residual noises in the waveform (see Fig. 7), the noise does not cause any baseline drifting to the signal but can be detected by the peak detection, which directly influences the impulse pairing for the unipolar charge signals.

To remove any error peak pairs, a threshold value was setup in the study. If the magnitude of any point pairs was less than

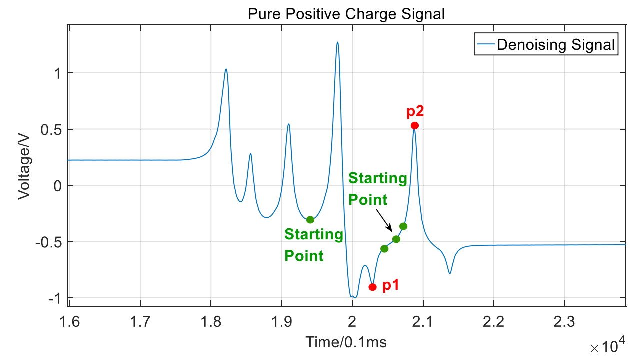

Fig. 8. Fake peaks and varied start points in a bipolar charge signal.

the threshold, the peaks were accounted as noise and ignored. The threshold value needs to be selected carefully according to the data, which can eliminate the noise without affecting the signal. Therefore, for unipolar charge, the amplitude and location of the true peaks can be obtained according to the filtered peak pairs without using baseline tracking.

B. Baseline Tracking for Bipolar Charge Signals

Baseline tracking for bipolar charge signals is much more complicated compared to the unipolar charge signals, as both positive and negative peaks are presented for peak detection. For a typical bipolar charge signal shown in Fig. 8 as an example, it is hard to judge whether the point p1 is a point between two positive peaks or a valid negative peak. Similarly, the point p2 could be either a valid positive peak or a transitional region of two negative peaks. This creates fake peaks, which needs to be identified before measuring it. The fake peaks in the signals are rarely mentioned in the literature, but they are crucial for determining the charges carried by particles in inductive charge sensors. So, baseline tracking is necessary for removal of any drifting in original signals in order to process the charge signals accurately.

To solve the 'fake peaks' problem, a new method of judging the shape of each peak is proposed in this paper. A standard templated signal for a single particle (for example, a positive peak) is used to compare with the waveform in a raw signal for multiple particles to extract position and amplitude of valid individual peaks. To analyze similarity between the template signals and the virgin signals from the sensor, the dynamic time warping algorithm is applied.

Because output of a dynamic time warping algorithm is an accumulative distance that reflects the difference between the two-time series, by the formula, this distance can be easily converted into similarity as:

$$\text{Similarity} = 1/(\text{Distance} + 1) \tag{3}$$

The advantage of the dynamic time warping algorithm is capability of comparing time series in different signal lengths, which is suitable for the peak comparison.

To achieve this, a single particle is firstly used to generate a standard charge signal, in which typical rise trend and drop trend are extracted as the template signals of a valid peak. The templates influence further baseline tracking and need to be done carefully. Fig. 9 shows typical rise and drop trends extracted from the signals of polymer and calcium carbonate.

Secondly, peak detection is performed on the original raw signals. By pairing the obtained adjacent positive and negative

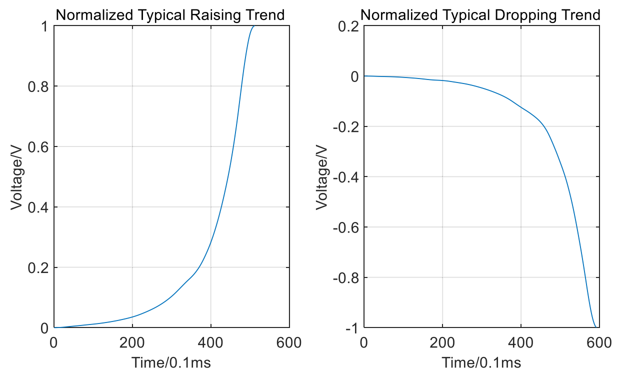

Fig. 9. Standard template signals of a true peak signal. Raising trend for polymer particle and dropping trend for calcium carbonate particle.

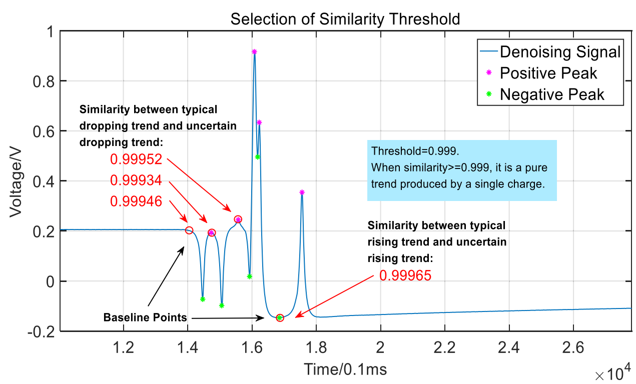

Fig. 10. Selection of similarity threshold.

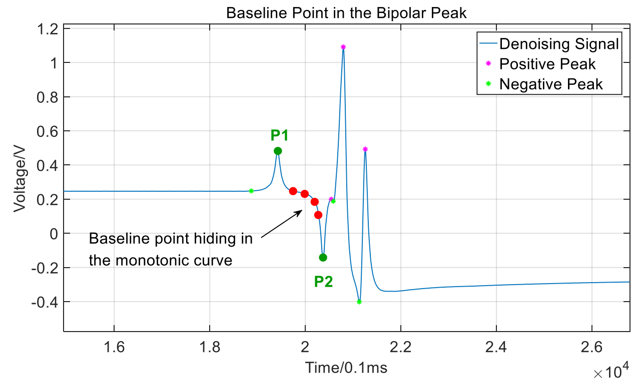

Fig. 11. Detecting baseline points in peaks of opposite polarity.

poles, the uncertain rising trends and dropping trends are detected. Considering that the amplitude of each peak is different, and the dynamic time warping algorithm is based on Euclidean distance, thus each uncertain trend needs to be normalized so that their amplitude is consistent with the template signal. Then, the similarity between uncertain trends and the template signals is compared by the dynamic time warping algorithm.

The results of a similarity comparison shown in Fig. 10 demonstrate that, the similarity between a template signal and a valid peak generated by a charge (true peaks) is always higher than 0.999. If the similarity is less than 0.999, it means a fake trend. With the experimental tests, it can be indicated that the value of 0.999 is the key threshold to distinguish a true peak in a raw signal. Although most of the trends are also very similar to the template signals (>0.99 in similarity), the baseline points can be distinguished when the similarity reaches 0.999, which proves that the dynamic time warping algorithm can achieve high accuracy in comparing the waveform shape, which can recognize the target signals.

If a monotonous trend between two poles is generated entirely by a single charge, it can be inferred that the previous peak is also of the same polarity as the present peak. The starting point of the present trend, then, is the transition point sandwiched between two homo-polar peaks. These points are the points on the baseline, and a rough baseline can be determined by the defined baseline points. However, there are still some baseline points hidden in between the peaks. Because the monotonous trend that contains a baseline point can have two situations, the baseline point can belong to a positive peak and a negative peak simultaneously.

To overcome this challenge, the waveform is divided into segments and then compared with the standard templated signal to locate the baseline points. As shown in Fig. 11, point p1 is a positive signal peak, and point p2 is a negative peak. On the monotonic curve from p1 to p2, taking p1 as a constant starting point, the trend in different lengths in the direction of p2 is taken and compared with the standard dropping trend. If the similarity between the downtrend of some segments and the standard signal is greater than 0.999, the endpoints of these downtrends (the red dot in the figure) are marked. After all subsets of a trend are compared, the abscissa of all marked points is averaged to calculate the position of the final baseline point.

By the way, two different types of baseline points can be detected. Although there is no guarantee that all the baseline points in a signal can be detected, the similarity threshold of 0.999 ensures the accuracy of the points already have been found. The baseline points can be used to form the baseline of the charge signal for further charge detection. To form the baseline in the signal, linear regression is used to create the fitting lines between the baseline points, because the number of baseline points in a signal are significant and creating fitting lines with polynomial regression is time-consuming. However, the baseline tracking obtained by a linear function between the baseline points can generate called 'humps' errors between the peaks after repositioning the points, which needs to be removed by a further process.

C. Reprocess the Problematic 'Humps' Errors

As identified, some slow drifting causes the 'humps' errors. Even with the DTW algorithm, fake signals cannot be removed completed in the processed signal after the baseline correction as shown in Fig. 12. These errors are obvious in shape compared to the peaks produced by the charges. So, evaluating sharpness of the peaks for peak shape comparison is applied to solve the problem as shown in Fig. 12.

The principle for sharpness comparison method is, a hump and a charge peak as shown in the figure, with a horizontal line, BC taken at the middle position of the amplitude (between the baseline point and the peak) and then getting the length AD from this line to the vertex. The sharpness of peaks is measured by the value of AD/BC. To identify a charge peak, the sharpness for a peak is less than a certain threshold. Otherwise, it is a hump. Generally, if the threshold is set to 4, most of humps can be identified. This threshold may need to change according to different materials. Although there are other methods that can be used for the 'humps' error removal, the sharpness comparison method is simplest and cheapest in computing time consumption. More thinking on baseline correction for the humps have been given as taking

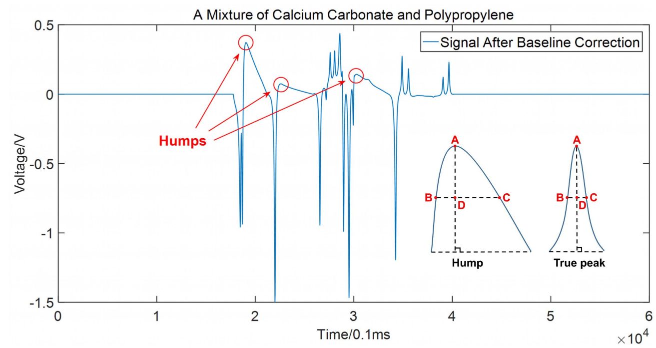

Fig. 12. Humps in processed signal and evaluation of the sharpness of the peak.

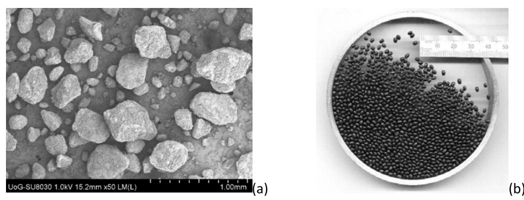

Fig. 13. (a) Calcium carbonate particles, (b) expanded polypropylene beads.

the trend changing rate and comparing it to particle velocity. This can be done in future study.

V. Experimental Results and Discussion

To evaluate the new baseline tracking method, experimental study has been carried out on an electrostatic inductive sensor developed at the Wolfson Centre [9]. The capacitance of the feedback capacitor in the sensor is 10pF. A signal is taken by a data acquisition in MATLAB with a sample rate of 10 kHz. The tests run for a period of 6 seconds while the material is fed into the sensor. The signal has been processed in MATLAB with the new algorithms developed, for charge levels (charge to mass ratio) and polarity determinations.

Two typical particulate materials are selected, which can produce unipolar positive and negative charge. One material is expanded polypropylene beads produced by JSP Corporation (ARP5920), producing negative charges. Particle size of the polymer beads is about 3-5 mm. The other material is calcium carbonate with size of 0.85-1.0 mm, producing positive charges. The materials are shown in Fig. 13.

All experiments have been carried out in a temperature and humidity-controlled room (25°C and 45%-50% RH). In the experiments, the particles are charged in a plastic container for the same vibration time so similar charge can be achieved. With a vibratory feeder, a selected number of particles are fed into the sensor, so a charge signal of the particles is obtained. In principle, number of the peaks in the signal must be equal to the number of particles. However, due to the limitation of feeding method that the particles may be not dispersed very well, the number of the peaks detected may be different to the number of the particles fed. Therefore, when evaluating the algorithm error, the number of the peaks in the signal accounted manually is compared to the algorithm result. The number of particles fed into the sensor is used as a reference.

The results in Fig. 14 and 15 are the signals for 20 calcium carbonate particles and 20 polymer-beads, respectively. In the signals, the red point is the positive pole corresponding to each peak, and the green point is the negative pole. The magnitude

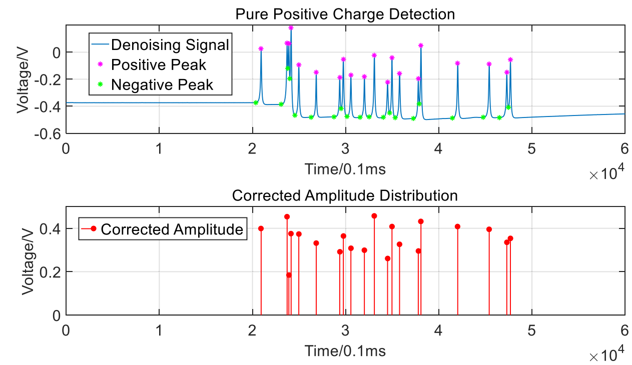

Fig. 14. The peaks detected for a positive charged signal of calcium carbonate.

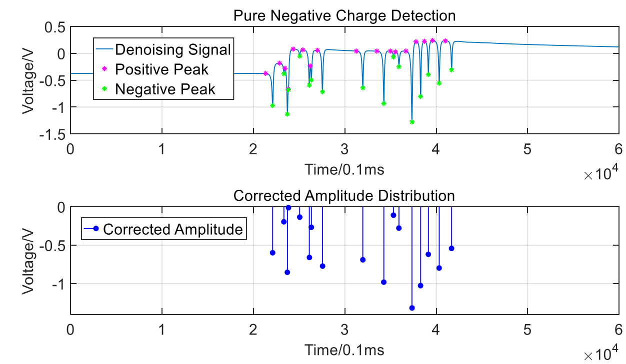

Fig. 15. The peaks detected for a positive charged signal of calcium carbonate.

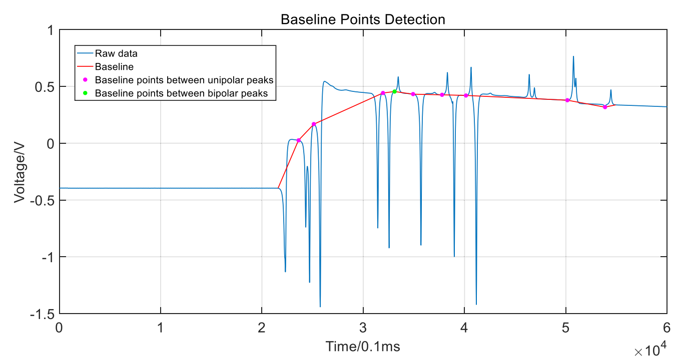

Fig. 16. Baseline points detected for a bipolar charged raw signal.

and distribution of the charge obtained by the algorithm are represented by a stem diagram. In Fig. 14, it shows 20 peaks detected from an output signal of the sensor and the amplitudes and positions in time domain corresponded to the raw signal.

In Fig. 15, only 17 peaks are detected in the original signal, and shown in the results given by the algorithm. By the error definition, there is no error for unipolar charge signal. If the threshold of noise is set reasonably, the algorithm will have minimum errors, as the algorithm can automatically detect every peak without any approximate processing.

Fig. 16 shows a bipolar charge signal obtained by mixing 10 calcium carbonate particles and 10 polypropylene beads. There are 8 positive and 9 negative peaks detected in the signal by the sensor. For the 17 peaks, 13 baseline points are detected and marked in red circles. These baseline points are connected by using a linear function to form a rough baseline.

With the baseline correction, the signal can be processed, and the drifting is removed (see Fig. 17). The 'humps' formed after baseline correction are detected by the sharpness method

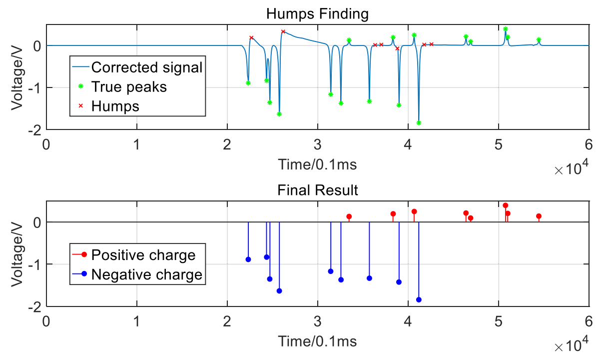

Fig. 17. Humps detection in processed signal.

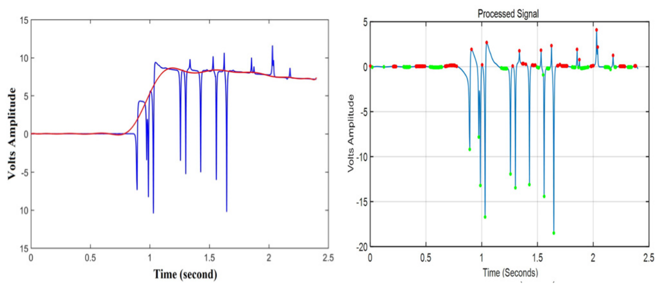

Fig. 18. The result of the baseline correction algorithm by Mazet [21].

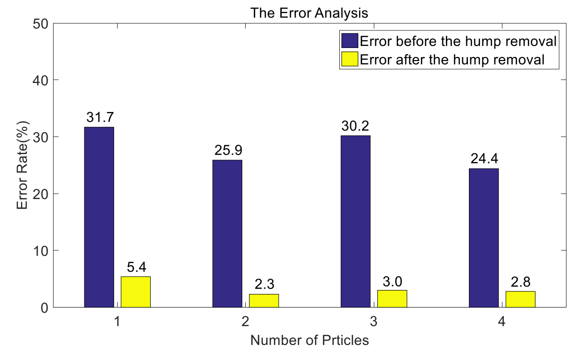

Fig. 19. The error analysis for different numbers of particles used in one detection.

and marked with red crosses, and the remaining true peaks are marked with green dots. The bottom diagram in Fig. 17 is the result after removing the humps, which shows that 8 positive and 9 negative peaks in the raw data are detected successfully.

It Fig. 18, it presents a result of the same signal using the baseline correction method proposed by Mazet *et al.* [21] as a comparison. The Mazet's method uses polynomial fitting to derive the baseline, and the polynomial order is estimated by minimizing a non-quadratic criterion. Comparing the results in Fig. 16, 17, and 18, it can be found that the baseline obtained by the Mazet's algorithm is quite rough at some key positions (such as the starting points of some peaks). The results by the Mazet's method also contain many fake detections when it deals with the subtle noise and the drifting, being miscounted for charge peaks. To remove the fake detections of the peaks, the current method has a great advantage.

For bipolar charge signals, the processed results still contain some errors as the proposed method only finds part of the baseline points to make a rough estimate of the baseline. To quantify the error and verify the repeatability of the algorithm, more experiments with a specific number of particles have been carried out, which four groups (the total number of particles are 20, 40, 60, and 100, respectively, contained the same number of calcium carbonate and polypropylene particles) are used. The error can be calculated by:

$$error = \frac{error_{pos}}{number_{pos}} \times \frac{number_{pos}}{number_{total}} + \frac{error_{neg}}{number_{neg}} \times \frac{number_{neg}}{number_{total}} = \frac{error_{pos} + error_{neg}}{number_{total}} \quad (4)$$

where $error_{pos}$ and $error_{neg}$ are the difference between the actual number of peaks and the number of peaks given by the algorithm for positive and negative charges.

From the experimental results (in Fig. 19), the error of the four signals before hump removal is about 25-30%, which is relatively high. However, after the hump removal, the error of the algorithm drops significantly. Especially when number of particles increases to more than 50, the error is dropped to within 3%. It suggests that the hump errors caused by an inappropriate baseline have a huge impact on the results. While focusing on the accuracy of baseline tracking, the proposed algorithm also generates many hump errors, but the errors can be reduced by the hump removal.

In addition, efficiency of the program developed has been evaluated and optimized. Because the dynamic time warping algorithm needs to build a cumulative distance matrix to obtain the similarity, in charge signals a single trend may contain thousands of data for a total 60,000 data in current single test. It is very time-consuming to generate a large cumulative distance matrix and calculating the values of the elements. In detection of baseline points between opposed-polarity peaks, the efficiency of the program is very poor when a high number of peaks are dealt with, and it may take hours to solve all the data. To improve the efficiency of the program, the detection interval is increased when the baseline points between the bipolar peaks are detected. Instead of traversing every data point, 20 evenly distributed data points are used on each trend, and one of the most suitable baseline points is selected. With the improvement, the processed results show the same accuracy as before, but the running time of the program is significantly reduced to less than five minutes.

To achieve a faster detection speed, the number of sampling points on a single trend can be reduced further, because 20 sampling points is still in a sufficiently accurate sampling range. Sample points can be set to 15 or 10 depending on the signals obtained, which can reduce the detection time further in a few seconds. This approach is flexible, which allows for trade-offs between accuracy and processing time by changing the sampling interval.

VI. Conclusion

Static charges measured by an inductive sensor are highly depended on baseline tracking in the signal process. The study shows that none of the exiting methods can deal with the complexity of bipolar charge signals in baseline tracking. A new baseline tracking method has been developed based on types of charge polarity in the charge signals.

For unipolar charge signals, the study shows that polarity and distribution of the signals can be obtained simply by calculating magnitude of the paired poles without baseline tracking. For any bipolar charge signals, variation of baseline points detected in between the opposed peaks prevents correct tracking. Therefore, a similarity comparison method between a standard charge template and a charge signal based on dynamic time warping (DTW) algorithm has been developed and show great advantages for baseline tracking of bipolar charge signals. However, ‘humps’ errors due to slow drifting in the signals result in huge errors. By an evaluating sharpness of peaks method, the experiment results show that the error rate of the algorithm in a detection can drop from about 30% down to about 3%.

One drawback of the proposed method is a large processing time due to the number of data points processed. With an acceptable accuracy, the time can be reduced by control of the data points or increasing the sampling interval. User-defined similarity thresholds and sampling intervals make this algorithm flexible. The study shows the similarity of 0.999 is key threshold to distinguish a true peak in a raw signal.

In the study, some further works are remaining. As selection of standard template signals for determining the threshold value used is crucial, selection criterions need to be studied for more situations to avoid any deviation in the selection. Also, other methods for hump errors removal in baseline correction need to be studied in future.

References

[1] J. Wong, P. C. L. Kwok, and H.-K. Chan, “Electrostatics in pharmaceutical solids,” *Chem. Eng. Sci.*, vol. 125, pp. 225–237, Mar. 2015.

[2] Y. Pu, M. Mazumder, and C. Cooney, “Effects of electrostatic charging on pharmaceutical powder blending homogeneity,” *J. Pharmaceutical Sci.*, vol. 98, no. 7, pp. 2412–2421, Jul. 2009.

[3] M. Glor, *Electrostatic Hazards in Powder Handling*. Letchworth, U.K.: Research Studies, 1988.

[4] J. R. Mountain, M. K. Mazumder, R. A. Sims, D. L. Wankum, T. Chasser, and P. H. Pettit, “Triboelectric charging of polymer powders in fluidization and transport processes,” *IEEE Trans. Ind. Appl.*, vol. 37, no. 3, pp. 778–784, May 2001.

[5] D. M. Taylor, “Measuring techniques for electrostatics,” *J. Electrostatics*, vols. 51–52, pp. 502–508, May 2001.

[6] R. Liu, S. Bei, and J. Zhou, “Research of structure and characteristics for tribological electrostatic sensors,” in *Proc. 3rd Int. Conf. Modeling, Simul. Appl. Math. (MSAM)*, 2018, pp. 325–328.

[7] S. Matsusaka, H. Maruyama, T. Matsuyama, and M. Ghadiri, “Triboelectric charging of powders: A review,” *Chem. Eng. Sci.*, vol. 65, no. 22, pp. 5781–5807, Nov. 2010.

[8] S. Matsusaka and H. Masuda, “Simultaneous measurement of mass flow rate and charge-to-mass ratio of particles in gas–solids pipe flow,” *Chem. Eng. Sci.*, vol. 61, no. 7, pp. 2254–2261, Apr. 2006.

[9] T. Hussain, “Novel approaches to signal acquisition and processing in relation to sensing electrostatic behaviour of particulate materials in motion,” Ph.D. dissertation, Dept. Eng. Sci., Univ. Greenwich, London, U.K., 2014.

[10] B. Raman, R. Shenoy, D. C. Meier, K. D. Benkstein, C. Mungle, and S. Semancik, “Detecting and recognizing chemical targets in untrained backgrounds with temperature programmed sensors,” *IEEE Sensors J.*, vol. 12, no. 11, pp. 3238–3247, Nov. 2012.

[11] K. Sothivelr, F. Bender, F. Josse, E. E. Yaz, A. J. Ricco, and R. E. Mohler, “Online chemical sensor signal processing using estimation theory: Quantification of binary mixtures of organic compounds in the presence of linear baseline drift and outliers,” *IEEE Sensors J.*, vol. 16, no. 3, pp. 750–761, Feb. 2016.

[12] S. U. Sigurdsson, R. Rupakhety, and R. Sigbjörnsson, “Adjustments for baseline shifts in far-fault strong-motion data: An alternative scheme to high-pass filtering,” *Soil Dyn. Earthq. Eng.*, vol. 31, no. 12, pp. 1703–1710, Dec. 2011.

[13] B. Maess, E. Schröger, and A. Widmann, “High-pass filters and baseline correction in M/EEG analysis. Commentary on: ‘How inappropriate high-pass filters can produce artefacts and incorrect conclusions in ERP studies of language and cognition,”’ *J. Neurosci. Methods*, vol. 266, pp. 164–165, Jun. 2016.

[14] Y. I. Jang, J. Y. Sim, J.-R. Yang, and N. K. Kwon, “The optimal selection of mother wavelet function and decomposition level for denoising of DCG signal,” *Sensors*, vol. 21, no. 5, p. 1851, Mar. 2021.

[15] G. Vega-Martinez, C. Alvarado-Serrano, and L. Leija-Salas, “ECG baseline drift removal using discrete wavelet transform,” in *Proc. 8th Int. Conf. Electr. Eng., Comput. Sci. Autom. Control*, Oct. 2011, pp. 1–5.

[16] B.-F. Liu, Y. Sera, N. Matsubara, K. Otsuka, and S. Terabe, “Signal denoising and baseline correction by discrete wavelet transform for microchip capillary electrophoresis,” *Electrophoresis*, vol. 24, no. 18, pp. 3260–3265, Sep. 2003.

[17] T. N. Pin, “An algorithm for quantile smoothing splines,” *Comput. Statist. Data Anal.*, vol. 22, no. 2, pp. 99–118, Jul. 1996.

[18] R. P. Goehner, “Background subtract subroutine for spectral data,” *Anal. Chem.*, vol. 50, no. 8, pp. 1223–1225, Jul. 1978.

[19] B. Jüttler, “Shape preserving least-squares approximation by polynomial parametric spline curves,” *Comput. Aided Geometric Des.*, vol. 14, no. 8, pp. 731–747, Oct. 1997.

[20] Y. Pang, L. Deng, J. Z. Lin, Z. Y. Li, G. Q. Li, and Q. N. Zhou, “Removal method of baseline drift from ECG signals based on morphology filter,” *Appl. Mech. Mater.*, vols. 427–429, pp. 1691–1695, Sep. 2013.

[21] V. Mazet, C. Carteret, D. Brie, J. Idier, and B. Humbert, “Background removal from spectra by designing and minimising a non-quadratic cost function,” *Chemometr. Intell. Lab.*, vol. 76, no. 2, pp. 121–133, Feb. 2005.

[22] R. Srivastava and P. Sinha, “Hand movements and gestures characterization using quaternion dynamic time warping technique,” *IEEE Sensors J.*, vol. 16, no. 5, pp. 1333–1341, Mar. 2016.

[23] Z. Zhang, T. Zhao, X. Ao, and H. Yuan, “A vehicle speed estimation algorithm based on dynamic time warping approach,” *IEEE Sensors J.*, vol. 17, no. 8, pp. 2456–2463, Apr. 2017.

[24] T. Syeda-Mahmood, D. Beymer, and F. Wang, “Shape-based matching of ECG recordings,” in *Proc. 29th Annu. Int. Conf. IEEE Eng. Med. Biol. Soc.*, Aug. 2007, pp. 2012–2018.

[25] B. Dainton, *Time and Space*. Ithaca, NY, USA: Mcgill-Queen’s Univ. Press, 2010, pp. 68–102.

[26] C. Myers, L. Rabiner, and A. Rosenberg, “Performance tradeoffs in dynamic time warping algorithms for isolated word recognition,” *IEEE Trans. Acoust., Speech, Signal Process.*, vol. ASSP-28, no. 6, pp. 623–635, Dec. 1980.

Yang Jiang received the B.Sc. degree from the School of Electrical Engineering, Yancheng Institute of Technology, Yancheng, China, in 2019, the B.Sc. degree from the School of Engineering, Faculty of Engineering and Science, University of Greenwich, U.K., in 2020, and the M.Sc. degree from The University of Edinburgh, U.K., in 2021. His research interests include signal processing algorithm and computer assisted measurements.

Tong Deng received the B.Sc. degree in physics from Liaoning University, Shenyang, China, in 1987, the B.Eng. degree in electromechanical engineering from Shenyang Science and Technology University, Shenyang, in 1992, the M.Sc. degree from The University of Manchester, U.K., in 1997, and the Ph.D. degree from the University of Greenwich, U.K., in 2001. He has been working as a Consultancy Engineer in Bulk Solids Handling Technology since 2001. He started his teaching and research contract at the School of Engineering in 2013. His research interests include characterization of powders and particle dynamics in material handling systems including electrostatic charges of particulates.

Karim M. Nasr (Senior Member, IEEE) received the Ph.D. degree from the University of Manchester, U.K., with a thesis on “Smart Antenna Systems for Wireless Networks.”

Before joining the University of Greenwich as a Senior Lecturer in Electrical Engineering, he was with the University of Manchester, Brunel University, BBC Research, NPL, Kingston University, and the University of Surrey (5GIC) investigating future wireless systems through a number of successful U.K. and European research projects. His main research interests include advanced signal processing techniques and wireless communication systems. He is a Chartered Engineer (C.Eng.), a member of the IET (MIET), the Institute of Physics (MInstP), and several European COST actions, a Senior Member of the European Association for Innovation (EAI), and a Fellow of the Higher Education Academy, U.K.